One-dimensional diffusion through single- and double-square barriers

1996 J. Phys. A: Math. Gen. 29 1567

(http://iopscience.iop.org/0305-4470/29/8/006)

J. Phys. A: Math. Gen. **29** (1996) 1567–1580. Printed in the UK

One-dimensional diffusion through single- and double-square barriers

V Berdichevsky and M Gitterman

Department of Physics, Bar-Ilan University, Ramat Gan 52900, Israel

Received 3 October 1995, in final form 18 December 1995

Abstract. Exact solutions are obtained for the diffusion through single- and double-square potentials, by using the Laplace transform method. We compare transmission of a classical particle through one barrier of given length and through two barriers with a well between them of the same overall length. The influence of the barriers' heights and widths as well as of the distances to the reflecting walls is studied in detail. The results obtained are used to estimate the limits of applicability of the Kramers rate theory.

1. Introduction

The transition between simultaneously stable states across a barrier is an old problem of great importance both in quantum and classical mechanics. The tunnelling of quantum particles through a potential barrier is a clearly understood quantum-mechanical problem [1]. One of the peculiarities of this problem is a comparison of the transition through a double barrier (figure 1(*b*)) and a single barrier (figure 1(*a*)). It turns out that the transmission coefficient for the incident particle can reach nearly unity for a double barrier even through each of the barriers has a low transparency. This resonance phenomenon takes place when the energy of an incident particle is close to one of the eigenstates of the potential well that divides the two barriers [1].

A classical particle with energy smaller then the barrier height is able to cross the barrier only in the presence of fluctuations. Such fluctuation-induced transitions are of great importance in physics, chemistry and biology [2]. The most often used approximation for the overdamped motion is due to Kramers [3]. A detailed survey of the fifty years of developments of this problem can be found in recent review articles [4, 5].

The Fokker–Planck equation for the overdamped motion can be solved exactly for the steady state and for some simple forms of potential also for the time-dependent case. The potentials shown in figure 1 belong to the class of simple potentials when the exact solution for the full dynamic problem can be obtained by using the Laplace transform method or by transferring the Fokker–Planck equation to the Schrödinger form [6]. We use the former method, focusing our attention, in particular, on a comparison between the potentials shown in figures 1(*a*) and (*b*), and investigate whether the existence of a potential well is able, as in the quantum-mechanical case, to assist the transmission over the barrier. We also try to extract all the possible information from the exact solution, including the validity of the Kramers rate theory and the dependence of the transmission on the barrier's heights and on the distance to the reflecting walls.

0305-4470/96/081567+14$19.50

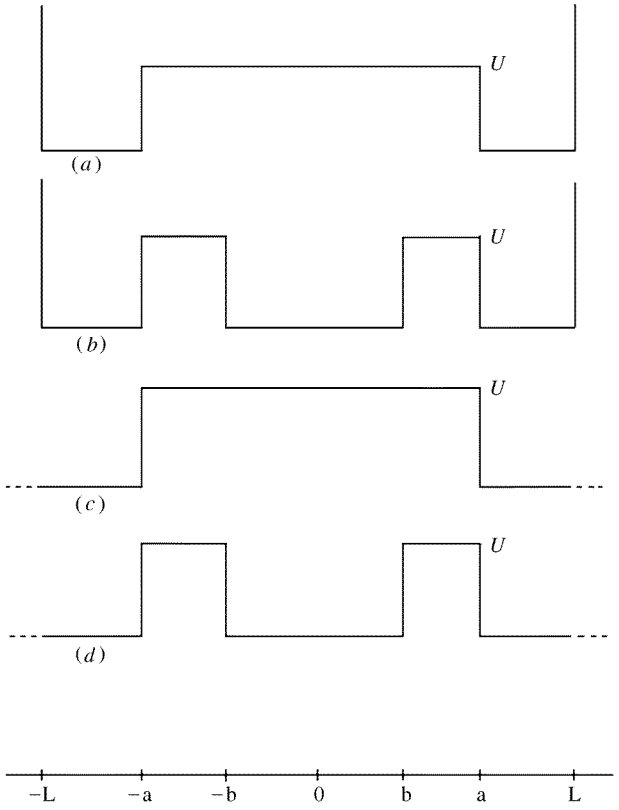

Figure 1. Different forms of square-well potentials: (*a*) one barrier of width $2a$ and height U with reflecting boundaries at $x = \pm L$; (*b*) two barriers of width $a - b$ and height U with a well of width $2b$ between the barriers and reflecting boundaries at $x = \pm L$; (*c*) the same as (*a*) with no boundaries; (*d*) the same as (*b*) with no boundaries.

2. Basic equations

The Fokker–Planck equation for the probability density function $P(x, t)$ for the position x of a diffusing particle at time t is

$$\frac{\partial P}{\partial t} = \frac{\partial}{\partial x}\left[\frac{1}{kT}\frac{\mathrm{d}U}{\mathrm{d}x}P + \frac{\partial P}{\partial x}\right] \equiv -\frac{\partial J}{\partial x} \tag{1}$$

where J is the probability current, and the diffusion coefficient is chosen equal to unity so that the time is measured in units of length squared. For the potentials shown in figure 1 $\mathrm{d}U/\mathrm{d}x = 0$, and (1) reduces to the simple diffusion equation. On performing the Laplace transform

$$\hat{P}(x, s) = \int_0^\infty P(x, t)\mathrm{e}^{-st}\,\mathrm{d}t \tag{2}$$

one can rewrite (1) in the following form:

$$s\hat{P} - P(x, 0) = \frac{\partial^2 \hat{P}}{\partial x^2}\,. \tag{3}$$

For simplicity we assume that initially a particle is located at the very left end of the barrier

$$P(x, t = 0) = \delta(x + a) \tag{4}$$

although it is physically obvious that all qualitative results will not depend on the precise initial position of the particle in the interval $(-L, -a)$.

Substituting (4) into (3) leads to the following equation:

$$\frac{\partial^2 \hat{P}}{\partial x^2} + \delta(x + a) = r^2 \hat{P} \qquad r = \sqrt{s}\,. \tag{5}$$

One can solve (5) in the three regions of interest for the potential shown in figure 1(*a*) and five regions for that in figure 1(*b*). In the former case the solutions of (5) are given by

$$\begin{aligned} \hat{P} &= C_1 \mathrm{e}^{rx} + C_2 \mathrm{e}^{-rx} \qquad -L < x < -a \\ \hat{P} &= C_3 \mathrm{e}^{rx} + C_4 \mathrm{e}^{-rx} \qquad -a < x < a \\ \hat{P} &= C_5 \mathrm{e}^{rx} + C_6 \mathrm{e}^{-rx} \qquad a < x < L \end{aligned} \tag{6}$$

and similar formulae can be written for the five regions in figure 1(*b*).

In both cases we assume reflecting boundary conditions at boundaries $x = L$ and $x = -L$ which means that the probability current vanishes at these points, $J(L, s) = J(-L, s) = 0$, i.e.

$$\begin{aligned} C_1 \mathrm{e}^{-rL} - C_2 \mathrm{e}^{rL} &= 0 \\ C_5 \mathrm{e}^{rL} - C_6 \mathrm{e}^{-rL} &= 0\,. \end{aligned} \tag{7}$$

The coefficients C_i are determined by the continuity of P and J at the points $x = \pm a$ and $x = \pm b$. Some caution has to be used due to jumps of potential at these points [6]. Continuity of the probability current J which according to equation (1) can be written as $J = -\mathrm{e}^{-U/kT} \frac{\partial}{\partial x}\left[\mathrm{e}^{U/kT} \hat{P}\right]$ means that at points z of the (finite) jumps of potentials

$$\begin{aligned} &\mathrm{e}^{U(z+0)/kT} \hat{P}(z + 0, s) - \mathrm{e}^{U(z-0)/kT} \hat{P}(z - 0, s) = 0 \\ &\frac{\partial \hat{P}(z + 0, s)}{\partial x} - \frac{\partial \hat{P}(z - 0, s)}{\partial x} = 0\,. \end{aligned} \tag{8}$$

The latter condition has an additional term (-1) at the point $x = -a$ which comes from the integration of $\delta(x + a)$ in (5) near $x = -a$.

Therefore, for the potential shown in figure 1(*a*) the matching conditions (8) for the distribution functions (6) take the form:

$$\begin{aligned} &C_1 \mathrm{e}^{-ra} + C_2 \mathrm{e}^{ra} = (C_3 \mathrm{e}^{-ra} + C_4 \mathrm{e}^{ra})\, \mathrm{e}^{U_0} \\ &C_1 \mathrm{e}^{-ra} - C_2 \mathrm{e}^{ra} - \frac{1}{r} = C_3 \mathrm{e}^{-ra} - C_4 \mathrm{e}^{ra} \\ &(C_3 \mathrm{e}^{ra} + C_4 \mathrm{e}^{-ra})\mathrm{e}^{U_0} = C_5 \mathrm{e}^{ra} + C_6 \mathrm{e}^{-ra} \\ &C_3 \mathrm{e}^{ra} - C_4 \mathrm{e}^{-ra} = C_5 \mathrm{e}^{ra} - C_6 \mathrm{e}^{-ra} \end{aligned} \tag{9}$$

and the analogous conditions can be written for the double barrier, figure 1(*b*). Here and later on we use the notation $U_0 = U/kT$.

The six equations (7), (9) determine the coefficients $C_1, \ldots, C_6$ and the analogous equations for two-barrier potential determine $C_1, \ldots, C_{10}$. Although we have analytical solutions for all coefficients C_i for our purposes we need only the coefficient C_5. Indeed, starting from the point $x = -a$ at $t = 0$ (see equation (4)) the Laplace transform of the

probability $W(t)$ of finding a particle in the region $[a, L]$ after crossing the barrier(s) is given by

$$\hat{W}(s) = \int_a^L \hat{P}(x, s)\,\mathrm{d}x = \frac{2C_5\,\mathrm{e}^{rL}}{r}\sinh(r(L-a)) \tag{10}$$

where the second of conditions (7) has been taken into account. After quite cumbersome calculations one can solve exactly the system of equations (7), (9). After substituting C_5 in (10) one gets

$$\hat{W}(s) = \frac{\mathrm{e}^{U_0}\sinh(2r(L-a))}{4r^2}\{\cosh(r(L-a))\cosh(ra) + \mathrm{e}^{U_0}\sinh(r(L-a))\sinh(ra)\}^{-1} \times \left\{\cosh(r(L-a))\sinh(ra) + \mathrm{e}^{U_0}\sinh(r(L-a))\cosh(ra)\right\}^{-1}. \tag{11}$$

Analogous, even more tedious, algebra gives the solution of a system of ten equations for the double-barrier potential:

$$\hat{W}(s) = \frac{\mathrm{e}^{2U_0}\sinh(2r(L-a))}{4r^2FG} \tag{12}$$

where the expressions F and G are of the form

$$\begin{Bmatrix} F \\ G \end{Bmatrix} = \left[\cosh(r(L-a))\sinh(r(a-b)) + \mathrm{e}^{U_0}\sinh(r(L-a))\cosh(r(a-b))\right]\begin{Bmatrix} \cosh(rb) \\ \sinh(rb) \end{Bmatrix} + \mathrm{e}^{U_0}\left[\cosh(r(L-a))\cosh(r(a-b)) + \mathrm{e}^{U_0}\sinh(r(L-a))\sinh(r(a-b))\right]\begin{Bmatrix} \sinh(rb) \\ \cosh(rb) \end{Bmatrix}. \tag{13}$$

It is obvious that in the limit $b \to 0$ the potential shown in figure 1(b) reduces to that in figure 1(a), and accordingly, (12) reduces to (11).

Two types of poles exist in (11) and (12): $r = 0$ which defines the asymptotic behaviour as $t \to \infty$, and those which come from the vanishing of A and B. One can easily find the asymptotic behaviour for one-barrier potentials with $L - a = na$, namely

$$W(t \to \infty) = \frac{\mathrm{e}^{U_0}}{2\left[\mathrm{e}^{U_0} + 1/n\right]}. \tag{14}$$

Since the inverse Laplace transform of (11) and (12) is not trivial we consider in the next section the special cases $n = 1$ and $n = \frac{1}{2}$ in (14) which simplify the inverse Laplace transform.

3. Some exact results

The simplest choice of the potential shown in figure 1(a) is

$$L = 2a\,. \tag{15}$$

Then the inverse Laplace transform of (11) has the following form:

$$W(t) = \frac{1}{2\pi\mathrm{i}}\frac{\mathrm{e}^{U_0}}{2(1+\mathrm{e}^{U_0})}\int_C \frac{\mathrm{e}^{st}\,\mathrm{d}s}{s\left[\cosh^2(ar) + \mathrm{e}^{U_0}\sinh^2(ar)\right]} \tag{16}$$

where C is the integration contour of the inverse Laplace transform, $s = \mathrm{Re}(s) + \mathrm{i}\sigma$ with fixed $\mathrm{Re}(s) > 0$ and the integral over σ is over $(-\infty, \infty)$.

The poles of the integrand in (16) are $s = 0$ with residue $2\pi\mathrm{i}$ and the values

$$s = -\frac{(\alpha + 2\pi n)^2}{a^2} \qquad r = \mathrm{i}\frac{\alpha + 2\pi n}{a} \qquad n = 1, 2, 3\ldots \tag{17}$$

where α is the root of the following equation:

$$\tan(\frac{\alpha}{2}) = \mathrm{e}^{-U_0/2} \tag{18}$$

To find the residues at these poles one gets

$$\begin{aligned} s\frac{\mathrm{d}}{\mathrm{d}s}\left[\cosh^2(ar) + \mathrm{e}^{U_0}\sinh^2(ar)\right]_{s=-\frac{(\alpha+2\pi n)^2}{a^2}} &= \frac{r}{2}\frac{\mathrm{d}}{\mathrm{d}r}\left[\cosh^2(ar) + \mathrm{e}^{U_0}\sinh^2(ar)\right]_{r=\mathrm{i}\frac{\alpha+2\pi n}{a}} \\ &= (\alpha + 2\pi n)\mathrm{e}^{U_0/2}\,. \end{aligned} \tag{19}$$

Equation (18) has been used in the last part of (19).

Hence, the probability $W(t)$ to be in the region (a, L) after crossing the barrier is

$$W(t) = \frac{\mathrm{e}^{U_0}}{2(1+\mathrm{e}^{U_0})} - \frac{\mathrm{e}^{U_0/2}}{1+\mathrm{e}^{U_0}} \sum_{n=-\infty}^{\infty} \frac{\exp\left(-\frac{(\alpha+2\pi n)^2}{a^2}t\right)}{\alpha + 2\pi n}\,. \tag{20}$$

The second term in (20) coincides with the result of calculation in [6] performed by transition from the Fokker–Planck equation to the Schrödinger equation while the first term was written in [6] as $\frac{1}{2}$ which coincides with (20) only for high barriers $U_0 \gg 1$.

The special choice (15) of the one-barrier potential leads to the simple result (20) since only one type of pole (17) exists in addition to the always existing pole $s = 0$ which defines the asymptotic behaviour of $W(t)$ as $t \to \infty$.

We bring now results of calculations similar to (17)–(19) for a different distance of the barrier from the reflecting wall, $L = \frac{3}{2}a$, where there appear two different types of poles. For

$$L = \tfrac{3}{2}a \tag{21}$$

one gets

$$\begin{aligned} W(t) = \frac{\mathrm{e}^{U_0}}{2(2+\mathrm{e}^{U_0})} + \frac{\mathrm{e}^{U_0}}{1+\mathrm{e}^{U_0}}\Bigg[&\frac{1}{(\mathrm{e}^{2U_0}+\mathrm{e}^{U_0})^{1/2}} \sum_{n=-\infty}^{\infty} \frac{\exp\left(-\frac{(\alpha_1+2\pi n)^2}{a^2}t\right)}{\alpha_1 + 2\pi n} \\ &- \frac{1}{(1+2\mathrm{e}^{U_0})^{1/2}} \sum_{n=-\infty}^{\infty} \frac{\exp\left(-\frac{(\alpha_2+2\pi n)^2}{a^2}t\right)}{\alpha_2 + 2\pi n}\Bigg] \end{aligned} \tag{22}$$

where

$$\cos(\alpha_1) = -\frac{1}{1+\mathrm{e}^{U_0}} \qquad \cos(\alpha_2) = \frac{\mathrm{e}^{U_0}}{1+\mathrm{e}^{U_0}}\,. \tag{23}$$

It is instructive to compare expressions (22) and (23) for the one-barrier potential shown in figure 1(*a*) with the appropriate two-barrier potential (figure 1(*b*)) obtained from (21) by adding an additional well at $-b < x < b$, namely

$$L = \tfrac{3}{2}a \qquad b = \tfrac{1}{2}a\,. \tag{24}$$

We now have to consider the poles in (13) with their residues, and then perform the inverse Laplace transform of (12). After calculations similar to (17)–(19) one obtains

$$\begin{aligned} W(t) = \frac{\mathrm{e}^{U_0}}{2(1+\mathrm{e}^{U_0})} + \frac{\mathrm{e}^{U_0}}{1+\mathrm{e}^{U_0}}\Bigg[&\frac{1}{(1+2\mathrm{e}^{U_0})^{1/2}} \sum_{n=-\infty}^{\infty} \frac{\exp\left(-\frac{(\alpha_1+2\pi n)^2}{a^2}t\right)}{\alpha_1 + 2\pi n} \\ &- \frac{\mathrm{e}^{U_0/2}}{(1+\mathrm{e}^{U_0}+\mathrm{e}^{2U_0})^{1/2}} \sum_{n=-\infty}^{\infty} \frac{\exp\left(-\frac{(\alpha_2+2\pi n)^2}{a^2}t\right)}{\alpha_2 + 2\pi n}\Bigg] \end{aligned} \tag{25}$$

where

$$\cos(\alpha_1) = \frac{e^{2U_0} - 2e^{U_0} - 1}{(1 + e^{U_0})^2} \qquad \cos(\alpha_2) = \frac{e^{2U_0} + 1}{(1 + e^{U_0})^2}\,. \tag{26}$$

For brevity we omit an additional exactly solvable case $L = \frac{4}{3}a$, $b = \frac{2}{3}a$.

The first terms in the right-hand sides of all expressions for $W(t)$ written above describe the asymptotic ($t \to \infty$) probabilities established after many reflections from the walls. One can easily show that the asymptotic probabilities to be in a given interval are proportional to the length of this interval multiplied by e^{-U_0} where U_0 is the potential barrier on this interval.

Hence, for the one-barrier potential shown in figure 1(a) the whole probability will be proportional to $2(L - a) + 2a\,e^{-U_0}$ and

$$W(t \to \infty) = \frac{L - a}{2(L - a) + 2a\,e^{-U_0}}\,. \tag{27}$$

Substituting in (27) $L = 2a$ and $L = \frac{3}{2}a$ one obtains the asymptotic terms in (20) and (22), respectively.

Analogously, for the two-barrier potential

$$W(t \to \infty) = \frac{L - a}{2(L - a) + 2b + 2(a - b)\,e^{-U_0}} \tag{28}$$

which reduces to the asymptotic term in equation (25) for $L = \frac{3}{2}a$ and $b = \frac{1}{2}a$.

One can also check that in the opposite limit case, $t = 0$, all the above equations for $W(t)$ are reduced to $W(t = 0) = 0$. To see this one has to use the summation formulae [7]:

$$\sum_{n=-\infty}^{\infty} \frac{1}{2n + \alpha} = \frac{\pi}{2} \cot\left(\frac{\pi\alpha}{2}\right). \tag{29}$$

To answer the question of whether the existence of a well inside a given barrier assists or inhibits the transmission through the barrier one has to compare (22) and (25). In all cases considered ($L = 2a$, $b = \frac{1}{2}a$; $L = \frac{4}{3}a$, $b = \frac{2}{3}a$; $L = \frac{3}{2}a$, $b = \frac{1}{2}a$) we calculated $W(t)$ and found that for all distances from the barrier to the wall, $L = 2a$, $L = \frac{3}{2}a$ and $L = \frac{4}{3}a$, the introduction of a well inhibits the transmission, i.e. it is easier to cross one barrier than two. However, the more detailed analysis in the subsequent sections will show that the last statement is not always correct.

4. Comparison with Kramers' escape rate

The exact results obtained in the last section can be compared with the well known Kramers formula for the rate of chemical reactions [3]. The rate of a thermally activated process is proportional to the Arrhenius factor $e^{-U/kT}$, where U is the height of a potential barrier. Kramers considered a Brownian particle moving in one dimension in an external field $U(x)$. He showed [3] that for high barriers, $U \gg kT$, when the rate of escape through the barrier is very small, this rate is defined mainly by the curvatures of the potential near its minimum and maximum. The latter assumption allows one to find the pre-exponential factor in the Arrhenius law, and to describe the jump rate across a barrier by a single rate exponent.

Different authors have checked the limits of applicability of the Kramers formula using the eigenvalues of a few known exact solutions of the Fokker–Planck equation [8–10], the concept of mean-free-passage time [11] or the Laplace transform method [12] (see the review paper [4]).

Let us first find the Kramers formula for the one-barrier potential shown in figure 1(*a*), where for brevity we denote the lengths of the three characteristic intervals from the left to the right by A_1, A_2 and A_3, and the points at the ends of the barrier's top by 1 and 2.

As follows from (1) one can rewrite the probability current J in the form

$$J = -\mathrm{e}^{-U_0}\frac{\partial}{\partial x}\left[\mathrm{e}^{U_0}P(x,t)\right]. \tag{30}$$

The main assumption in the Kramers theory of rates is the smallness of the time changes of the probability distribution function $P(x,t)$ and the probability current J which allows one to consider J for this quasi-stationary state as independent of x. Using the latter assumption one can integrate (30) with respect to x along the top of the barrier between points 1 and 2 which gives

$$P_2 - P_1 = J \cdot A_2\,. \tag{31}$$

The probability to be in regions A_1 and A_3 can be written as $A_1P_1\mathrm{e}^{U_0}$ and $A_3P_2\mathrm{e}^{U_0}$, respectively, where we used the jump condition (8) for P. Since $U_0 \gg 1$ one can neglect the particles sitting on the top of the barrier in the normalization condition which, therefore, will have the following form:

$$A_1P_1\,\mathrm{e}^{U_0} + A_3P_2\,\mathrm{e}^{U_0} = 1\,. \tag{32}$$

Combining equations (31) and (32) one gets

$$\frac{1}{J}\left[A_1P_1\,\mathrm{e}^{U_0} - \frac{A_1}{A_1+A_3}\right] = \frac{A_1A_2A_3}{A_1+A_3}\,\mathrm{e}^{U_0} \equiv \frac{1}{k_{r,1}}\,. \tag{33}$$

The expression in the brackets on the left-hand side of this formula defines the excess probability (above the equilibrium one) to find a particle in the region A_1. However, in the framework of the Kramers theory this probability times the rate $k_{r,1}$ defines the probability current J. Finally, coming back to our original notation, $A_1 = A_3 = L - a$ and $A_2 = 2a$, one finds that

$$k_{r,1} = \frac{\mathrm{e}^{-U_0}}{(L-a)a}\,. \tag{34}$$

The Kramers rate $k_{r,2}$ for the two-barriers potential shown in figure 1(*b*) can be found from analogous considerations. It turns out that one again obtains equation (33) with $A_1 = A_3 = L - a$ and $A_2 = 2(a-b)$, i.e.

$$k_{r,2} = \frac{\mathrm{e}^{-U_0}}{(L-a)(a-b)}\,. \tag{35}$$

Hence, in the Kramers approximation the rate is determined by the width of the barriers $2(a-b)$ rather than by that of the well between the two barriers. This latter result is, in fact, confirmed by the form of brackets in (33) which contains only the parameters of the region adjoining the reflecting walls.

A comparison of (34) and (35) with the exact results obtained in the previous section and with the general Laplace transform results of section 2 allows one to set a limit of applicability of Kramers rate theory. First of all, one can find the smallest eigenvalues for all cases considered in section 3. To this end one has to consider the $n = 0$ terms in the sums over n in (20), (22) and (25) which give $\alpha^2/4a^2$, $\alpha_2^2/4a^2$ and α_2^2/a^2, respectively. Afterwards, one finds the series in e^{-U_0} in the transcendental equations (18), (23) and (26) for these α. The results of these calculations up to $\mathrm{O}(\mathrm{e}^{-2U_0})$ are shown in the second column of table 1, and these should be compared with the first column which contains the Kramers formulae (34) and (35) for the appropriate values of L, a and b. The comparison of columns

I and II shows that for all the barriers considered the Kramers rates coincide with the main term in the expansion of the (exact) smallest eigenvalues while the next terms in column II provide, for high barriers, $U_0 \gg 1$, only small corrections to the Kramers results.

Since we have the exact formulae (11) and (12), (13) for the Laplace transform of the probability $W(t)$ to be in the region (a, L) after crossing the barrier, the possibility exists of comparing the Kramers formulae (34) and (35) with the appropriate rates obtained from (11) and (13) after expanding these equations in a small parameter e^{-U_0}. After some simple but tedious calculations one gets

$$k = \frac{e^{-U_0}}{(L-a)(a-b)} - \frac{(L-a+4b)(L^2-2aL+2a^2)-ab(3a+2L)+b^2(L+a-3b)}{(L-a)^3(a-b)^2}\, e^{-2U_0} + \cdots . \tag{36}$$

Needless to say, for appropriate L, a and b equation (36) gives the results of column 2 in table 1. One can see, however, that for all $L > a > b$ the second term remains smaller than the first one which justifies the Kramers rate theory. In deriving (36) we have assumed that the barriers are not too narrow, i.e $a - b = O(1) \gg e^{-U_0}$. Otherwise, the results would be quite different. For $a - b = O(e^{-U_0})$ the Arrhenius factor will disappear, and the whole picture will be quite different from that of Kramers, which is not so surprising since in Kramers' theory only one small parameter, e^{-U_0}, exists.

Another form of a single-exponent expression different from the Kramers rate was noted in [6]. The probabilities $W(t)$ may be approximated by a single potential

$$W_a(t) = W(t=\infty)[1 - e^{-rt}] \tag{37}$$

where the decay rate r is determined from the integral condition of the equal area of the exact expression $W(t)$ founded in section 3 and $W_a(t)$ defined by (37), i.e.

$$\int_0^\infty W_a(t)\,dt = \int_0^\infty W(t)\,dt . \tag{38}$$

Integration over t in (38) can be performed in a straightforward manner while for the calculation of sums over n on the right-hand side of these equations one can use the following formula [7]:

$$\sum_{n=-\infty}^{\infty} \frac{1}{(\alpha+2\pi n)^3} = \frac{1}{8}\cot\left(\frac{\alpha}{2}\right)\left[1+\cot^2\left(\frac{\alpha}{2}\right)\right]. \tag{39}$$

Table 1. Comparison of the transition rates for one- and two-squared high barriers ($U_0 \gg 1$) of different lengths obtained by the exact solution (column I), from the Kramers theory (column II) and by the 'equal area' rule (column III).

L	a	b	No of barriers	I	II	III
$\frac{4}{3}a$	a	0	1	$(3/a^2)\exp(-U_0)$	$(3/a^2)\exp(-U_0) - (10/3a^2)\exp(-2U_0)$	$(3/a^2)\exp(-U_0)$
$\frac{4}{3}a$	a	$\frac{2}{3}a$	2	$(9/a^2)\exp(-U_0)$	$(9/a^2)\exp(-U_0) - (24/a^2)\exp(-2U_0)$	$(27/5a^2)\exp(-U_0)$
$\frac{3}{2}a$	a	0	1	$(2/a^2)\exp(-U_0)$	$(2/a^2)\exp(-U_0) - (5/3a\exp(-2U_0))$	$(2/a^2)\exp(-U_0)$
$\frac{3}{2}a$	a	$\frac{1}{2}a$	2	$(4/a^2)\exp(-U_0)$	$(4/a^2)\exp(-U_0) - (20/3a^2)\exp(-2U_0)$	$(8/3a^2)\exp(-U_0)$
$2a$	a	0	1	$(1/a^2)\exp(-U_0)$	$(1/a^2)\exp(-U_0) - (2/3a^2)\exp(-2U_0)$	$(1/a^2)\exp(-U_0)$
$2a$	a	$\frac{1}{2}a$	2	$(2/a^2)\exp(-U_0)$	$(2/a^2)\exp(-U_0) - (11/3a^2)\exp(-2U_0)$	$(3/2a^2)\exp(-U_0)$

The final step will be an expansion in e^{-U_0} of all formulae of section 3 which define α—the procedure already used in obtaining the second column of table 1. For all cases considered the rates r obtained from the 'equal area' rule are shown in the third column of table 1. It turns out that these rates coincide with the exact result for the one-barrier but are different for the two-barrier potential.

5. Asymptotic expansions for small and large time

As we have seen in section 3, the full dynamic solution can be found analytically only for special relations between the characteristic lengths. However, one can estimate the asymptotic behaviour with time based on the general formulae (11) and (12) for one and two barriers, respectively.

Let us start with small t, confining our attention mostly to a comparison between one and two barriers. Assuming that the reflecting walls are comparatively far away so that $L-a > a-b, b$ one obtains in the leading order for one barrier

$$W(t) \approx \frac{2e^{-U_0}}{(1+e^{-U_0})^2}\,\mathrm{erfc}\left(\frac{a}{\sqrt{t}}\right) \approx \frac{2\,e^{-U_0}}{(1+e^{-U_0})^2}\sqrt{\frac{t}{\pi a}}\,e^{-a^2/t} \tag{40}$$

and for two barriers

$$W(t) \approx \frac{8\,e^{-2U_0}}{(1+e^{-U_0})^4}\,\mathrm{erfc}\left(\frac{a}{\sqrt{t}}\right) \approx 2\left[\frac{2e^{-U_0}}{(1+e^{-U_0})^2}\right]^2 \sqrt{t\pi a}\,e^{-a^2/t} \tag{41}$$

where the asymptotic expression for $\mathrm{erfc}(z)$ has been used [7].

On comparing (40) and (41) one concludes that they become identical only for $U_0 = 0$ as it should be. However, for both low ($U_0 \ll 1$) and high ($U_0 \gg 1$) barriers (41) is always smaller than (40), i.e. at least at small times before the reflection from the walls becomes important, it is easier to pass one barrier then two successive barriers. One notable exception is the case of low ($U_0 \ll 1$) and very narrow ($a-b$ is much smaller than a) barriers for which it can be shown that it is easier to pass two narrow barriers than one wide barrier.

Let us now turn our attention to the asymptotics for large t. For $t \to \infty$ the stationary distribution for two barriers has the following form (as was shown in section 3):

$$W(t=\infty) = \frac{e^{U_0}(L-a)}{2\left[e^{U_0}(L-a)+a+b(e^{U_0}-1)\right]}\,. \tag{42}$$

As one can see from (42) conversion to the case of one barrier, $b \to 0$, reduces (42) to (27) and results in an increase of the probability to cross the barrier. The explanation of this phenomenon is clear. Indeed, the stationary probability to be in the region $(-b, b)$ is higher in the two-barrier case (there is no barrier in this region), and, hence, the probability to be in the region of interest (a, L) is smaller compared with the one-barrier potential.

The limit form of (42) becomes particularly simple when the height of the barriers is very low, $U_0 \approx 0$, or they become very narrow, $b \to a$. In both these cases

$$W(t=\infty) = \frac{L-a}{2L} \tag{43}$$

i.e. the probability to be in some interval is determined only by the length of this interval. The probability to be on very high barriers is very small, and, therefore, for $U_0 \to \infty$

$$W(t=\infty) = \frac{L-a}{2(L-a+b)} \tag{44}$$

i.e. it is again determined by the length of the interval.

The first correction terms to (42) are proportional to $t^{-3/2}$. They are quite cumbersome, and we bring here results only for the one-barrier potential:

$$W(t)\mid_{t\to\infty} = W(t=\infty)\left[1 - \frac{La(L-a)(3e^{U_0}(L-a)-(L-5a))}{3\pi^{1/2}(e^{U_0}(L-a)+a)}t^{-3/2}\right]. \tag{45}$$

Let us summarize the results obtained in this section. When two barriers are not very low and very narrow it is easier to cross one barrier than two both for small and large t (figure 2). The non-trivial behaviour which we discuss in detail in the next section is observed for the intermediate t where it is easier to cross two barriers than one (figure 2), i.e. there are two intersections, A and B, of $W(t)$ for the one and two barrier potentials.

The results are different for low ($U_0 \ll 1$) and very narrow ($a-b$ is much smaller than a) barriers. As shown in figure 3, for small t, $W(t)$ for two barriers is larger than that of one barrier, and only one intersection point C exists.

6. Influence of reflecting walls and barriers' heights

From the asymptotic analysis for large and small times in the previous section one might gather the impression that it is always easier to cross a one-barrier potential than that of two

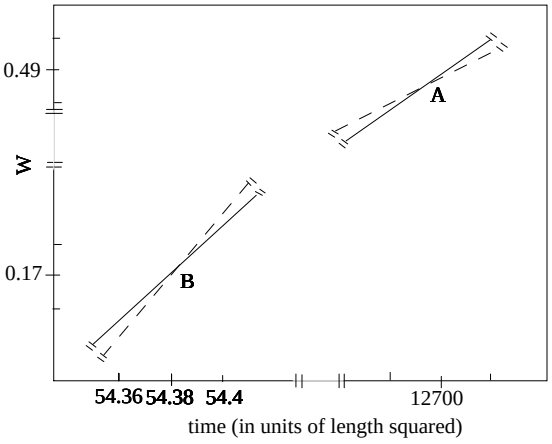

Figure 2. Time dependence of the probability to find a particle in the interval (a, L) after crossing one barrier (figure 1(*a*)): $L = 100$, $a = 3$, $b = 0$ (full curve) and two barriers (figure 1(*b*)): $L = 100$, $a = 3$, $b = 0.1$ (broken curve).

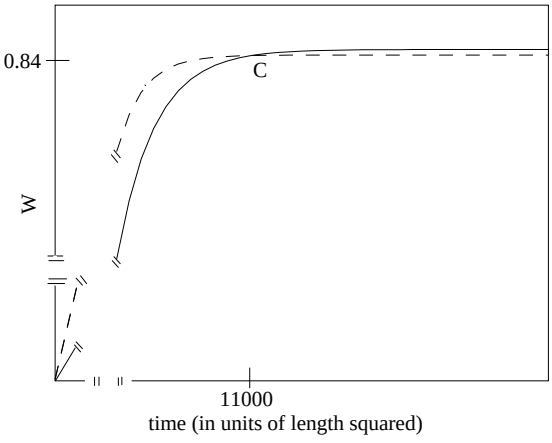

Figure 3. Time dependence of the probability to find a particle in the interval (a, L) after crossing low and very narrow barriers: one barrier, $L = 100$, $a = 3$, $b = 0$, $e^{U_0} = 5$ (full curve); two barriers, $L = 100$, $a = 3$, $b = 2.99$, $e^{U_0} = 5$ (broken curve).

barriers (except for the special case of very low and narrow barriers). However, physical intuition contradicts such an impression. Indeed, it seems easier to cross two narrow barriers ($|a-b|$ small—it does not have to be especially low and extremely narrow) than one wide barrier $(-a, a)$ of the same height. In order to clarify this point let us consider the potential without reflective walls or walls so far removed that a particle does not reach them even for asymptotically large t (figures 1(*c*), (*d*)).

The general approach to the solution of one-dimensional diffusion in the potential field shown in figures 1(*c*), (*d*) is very similar to the solution of the analogous problem depicted in figures 1(*a*) and (*b*). The only difference is that instead of reflecting boundary conditions (7) one now requires the finite value of the probability density function at $x \to \pm\infty$ which, in turn, results in $C_2 = C_5 = 0$ in (6), (7) and (9). We will not repeat the calculations performed in section 3, but rather bring here, as an example, the exact result for the probability $W(t)$ to cross one barrier (figure 1(*c*)):

$$W(t) = \frac{2\mathrm{e}^{U_0}}{(1+\mathrm{e}^{U_0})^2} \sum_{n=0}^{\infty} \tanh^{2n}\left(\frac{U_0}{2}\right) \operatorname{erfc}\left(\frac{a(2n+1)}{\sqrt{t}}\right). \tag{46}$$

Analogous to calculations of the previous section one can consider the asymptotic behaviour at large t for the two-barrier potential shown in figure 1(*d*). One gets for arbitrary values of a and b the probability to find a particle somewhere to the right of the barriers at large t

$$W(t) = \frac{1}{2} - \frac{1}{\sqrt{\pi t}} \left[a\cosh(U_0) - b(\cosh(U_0) - 1)\right]. \tag{47}$$

Note that the first correction terms are proportional to $t^{-1/2}$ while for barriers with reflecting walls the appropriate terms were proportional to $t^{-3/2}$. Moreover, passing in (47)

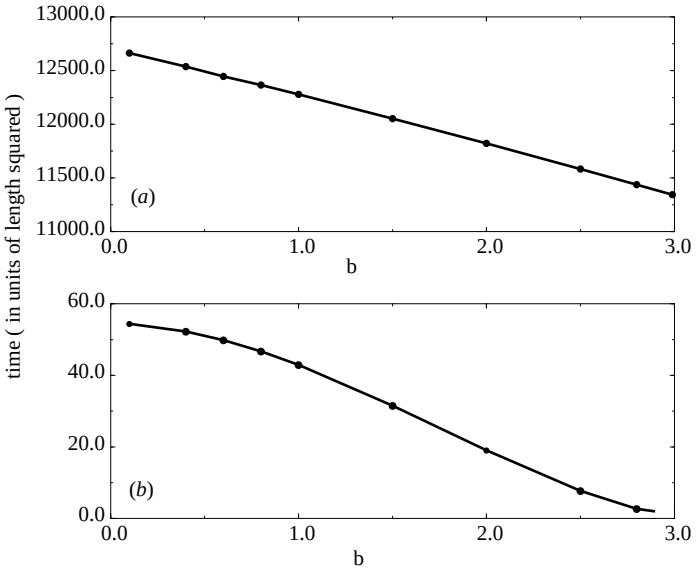

Figure 4. Characteristic times (in relative units) which define the intersections of two curves for one and two barriers with $L = 100$, $\mathrm{e}^{U_0} = 5$ and $a = 3$ as a function of the half-width of the well: (*a*) the large-time intersections (point A in figure 2); (*b*) the small-time intersections (point B in figure 2).

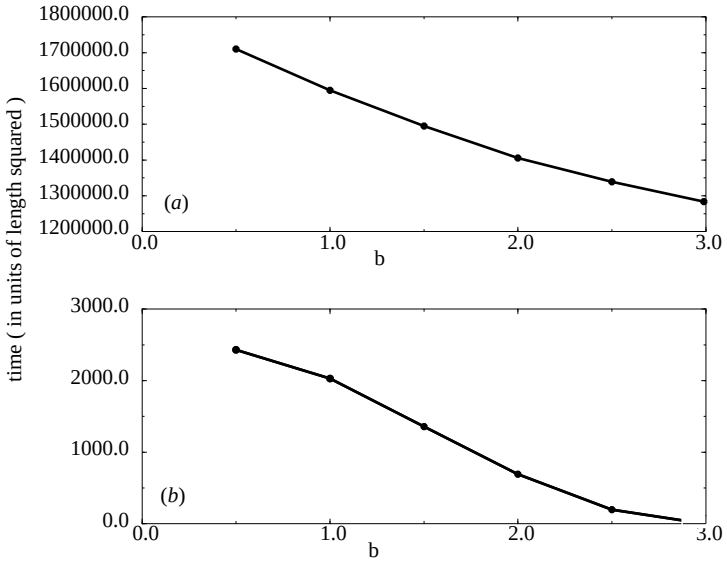

Figure 5. Characteristic times (in relative units) which define the intersections of two curves for one and two barriers with $L = 200$, $e^{U_0} = 500$ and $a = 3$ as a function of the half-width of the well: (*a*) the large-time intersections (point A in figure 2); (*b*) the small-time intersections (point B in figure 2).

to the case of one barrier, $b \to 0$, one can see that, in contrast to the results of the previous section, it is easier now to pass two barriers than one!

One can, however, imagine the following transition from the potential shown in figure 1(*b*) to that of figure 1(*d*). If one assumes that both the thicknesses of the barriers, $|a - b|$, and the distance between the barriers, $2b$, in figure 1(*b*) are very small compared to the distances to the reflecting wall, one obtains effectively the potential shown in figure 1(*d*) (apart from in the limit of $t \to \infty$). Hence, one can assume that for intermediate times it will be easier to cross two narrow barriers than one barrier. The walls for the barriers considered in section 3 were not far enough removed from the barriers. Therefore, we performed numerical calculations for far removed reflecting walls ($L = 200$ and $L = 100$ for $a = 3$) using different heights of the potential barrier, $e^{U_0} = 5$ and $e^{U_0} = 500$. We obtained the graphs shown in figures 4 and 5. In figures 4(*a*), (*b*) and 5(*a*), (*b*) one can see two intersection points, A and B, as functions of the half-size b of the well between two barriers. Points A in figures 4(*a*) and 5(*a*) are related to large t, and, in fact, the right part of these graphs already describes the points C in figure 3 for the narrow barriers, $a - b < a$. The points B in figures 4(*b*) and 5(*b*) define the second intersection points in figure 2, and they do not exist for narrow barriers in full agreement with figure 3.

Let us now consider the influence of the barrier heights on the transmission of a particle through these barriers. The probability of transmission has to be a non-monotonic function of the barrier height for large enough fixed times. In other words, for each given time there are two barrier heights with equal probability to cross them while for some intermediate height the transmission is maximal. This result is correct for both one and two barriers. For $U_0 = 0$ there is some probability to be in the region of interest (a, L) proportional to the length of this region. For larger U_0 there will be the smaller probability to find a particle in the region of the barriers, and, therefore, the probability to be in (a, L) will be

larger. Therefore the graph $W(U_0)$ grows linearly for small U_0. On the other hand for very large U_0 the probability to cross the barrier is very small. Therefore, the graph $W(U_0)$ must reach a maximum somewhere for the intermediate barrier heights. As an example, we show in figure 6 a graph of (25) depicting the probability $W(t)$ of finding a particle in the region (a, L) after crossing the barrier(s) as a function of the barrier height, e^{U_0} (in the exponential scale) for given fixed time $t = 100$ for a typical case $L = \frac{3}{2}a$ and $b = \frac{1}{2}a$. One can see from this figure that for both one and two barriers $W(t)$ has a maximum for some intermediate barrier height. The curves for one- and two-barrier potentials have a similar form, although the transmission for one barrier is higher especially for high barrier(s) as one would expect.

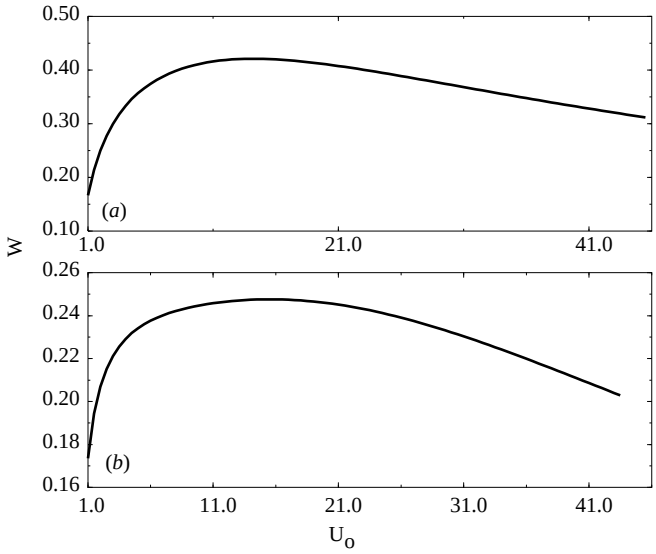

Figure 6. Probability $W(t)$ of finding a particle in the region (a, L) after crossing the barrier(s) as a function of the barrier height, e^{U_0} (in the exponential scale) for given fixed time $t = 100$ and: (a) $L = \frac{3}{2}a$, $b = 0$; (b) $L = \frac{3}{2}a$, $b = \frac{1}{2}a$.

7. Conclusions

We have performed a quite comprehensive analysis of one-dimensional motion in a very simple field consisting of single- or double-square barrier potentials. Surprisingly enough, the study of such a simple case allows one to obtain a few interesting results:

(i) Using the Laplace transform method we found the exact solutions for the probability $W(t)$ to be in the after-barrier(s) region when all characteristic lengths are ratios of simple integers. The asymptotic solutions for large and small t were found for arbitrary lengths.

(ii) We performed a comparison of transmission through one barrier of length $2a$ (figure 1(a)—case one) and two barriers with a well between them of the same overall length $2a$ (figure 1(b)—case two). It turns out that

(a) For unbounded motion (figure 1(c), (d)) the transmission is higher in case one for small t and in case two for large t.

(b) For restricted motion between two reflected walls when the barriers are not too narrow the transmission in case one is higher than in two both for large and small t.

However, for intermediate time it is easier to cross two barriers than one (figure 2). If two barriers are very narrow and low then the situation becomes similar to the unbounded motion (figure 1(*c*), (*d*)). Therefore, there are, in general, two intersection points between curves $W(t)$ for cases one and two, and only one point for very narrow barriers (figures 4 and 5).

(iii) For each given time $W(t)$ for reflecting walls is a non-monotonic function of the barrier height U_0, i.e. there are two barrier heights with equal probability to cross them, while for some intermediate height the transmission is maximal (figure 6).

(iv) We compared our exact results with the Kramers rate theory. It turned out that for high barriers the Kramers rates coincide with exact results in the leading order in e^{-U_0}, and small corrections appear in the next order (table 1). As expected, the Kramers theory does not work for very narrow barriers.

Acknowledgments

We are grateful to Jim Kiefer and Igor Khalfin for useful discussions and to the Israel Scientific Foundation for financial support.

References

[1] Merzbacher E 1986 *Quantum Mechanics* (New York: Wiley)
[2] Moss F and McClintock P (ed) 1989 *Noise in Nonlinear Dynamics Systems* vol 1–3 (Cambridge: Cambridge University Press)
[3] Kramers H 1940 *Physica* **7** 284
[4] Hanggi P, Talkner P and Borkovec M 1990 *Rev. Mod. Phys.* **62** 251
[5] Melnikov V 1991 *Phys. Rep.* **209** 1
[6] Mörsch M, Risken H and Volmer H D 1979 *Z. Phys.* B **32** 245
[7] Gradshtein I S and Ryzhik I M 1980 *Tables of Integrals, Series and Products* (New York: Academic)
[8] Larsen R S and Kostin M D 1978 *J. Chem. Phys.* **69** 4821
[9] van Kampen N G 1977 *J. Stat. Phys.* **17** 71
[10] Edholm O and Leimar O 1979 *Physica* **98A** 313
[11] Schutter K, Schutter Zan and Szabo A 1981 *J. Chem. Phys.* **74** 4426
[12] Frish H L, Privman V, Nicolis C and Nicolis G 1990 *J. Phys. A: Math. Gen.* **23** 1147